

## Mechanism of electrical conductivity of transparent $\text{InGaZnO}_4$

Masahiro Orita and Hiroaki Tanji

*R&D Center, HOYA Corporation, 3-3-1 Musashino, Akishima, Tokyo 196-8510, Japan*

Masataka Mizuno and Hirohiko Adachi

*Department of Materials Science and Engineering, Kyoto University, Sakyo, Kyoto 606-8501, Japan*

Isao Tanaka

*Department of Energy Science and Technology, Kyoto University, Sakyo, Kyoto 606-8501, Japan*

(Received 1 April 1999; revised manuscript received 2 September 1999)

The electronic structure of  $\text{InGaZnO}_4$ , which has a layered structure with alternating laminated layers of  $\text{InO}_2$  and  $\text{GaZnO}_2$ , was calculated in order to investigate the mechanism of electrical conductivity. In the crystal structure obtained through relaxation calculations using classical two-center potentials, the Ga ion in the  $\text{GaZnO}_2$  layer has pentagonal coordination forming a bipyramid with five oxygen ions, while the Zn ion in the same layer has tetrahedral coordination, losing a bond with the oxygen at the top of one pyramid. The molecular orbitals of model clusters for the relaxed structure, which were calculated by the discrete variational  $X\alpha$  method using a model cluster, show strong two-dimensional structures. The electronic states at the edge of the conduction band are the result of overlapping between In  $5s$  orbitals, and delocalize in the  $\text{InO}_2$  layer. The energy in the Ga  $4s$  and Zn  $4s$  states in the  $\text{GaZnO}_2$  layer was too large to be doped with electrons. The In  $5s$  states are considered to be conduction paths for carrier electrons. A very high conductivity can be expected in the case where dopant ions are introduced into the  $\text{GaZnO}_2$  layers.

### I. INTRODUCTION

Some oxides of  $p$ -block metals such as  $\text{ZnO}$ ,  $\text{In}_2\text{O}_3$ , and  $\text{SnO}_2$  feature both transparency for visible light and electrical conductivity. The electronic structure of these crystals is characterized by a wide band gap of over 3.0 eV, and highly concentrated donor levels of oxygen defects just below the conduction band.<sup>1</sup> The wide gap causes transparency in the visible region, and electrons at the shallow donor levels provide electrical conductivity. In the case of  $\text{In}_2\text{O}_3$ , it has been reported that a bulk single crystal has conductivity of 0.10 S/cm and mobility of 160  $\text{cm}^2/\text{V s}$  at room temperature.<sup>2</sup> The conductivity of  $\text{In}_2\text{O}_3$  can be increased significantly through doping with electrons by introducing a solution of Sn ions into the lattice (the Sn ions generate dense donor levels at the edge of the conduction band). The density of carriers can be increased to as much as  $1 \times 10^{21}/\text{cm}^3$ , while mobility is decreased significantly due to the scattering of electrons by the doped Sn ions.<sup>3</sup> Due to the tradeoff between carrier density and mobility, the maximum conductivity is limited to approximately  $1 \times 10^4$  S/cm.<sup>4</sup> A similar relationship is known to exist for  $\text{ZnO}$  and  $\text{SnO}_2$ , which have slightly lower maximum conductivities.

In the case of the tin-doped  $\text{In}_2\text{O}_3$  (ITO), conductive electrons are scattered by the tin ions distributed uniformly in the lattice. If it were possible to separate the tin ions from the space in which conductive electrons move, a high carrier density without a significant decrease in mobility could be realized.<sup>5</sup> We refer to this effect as "spatial separation" because the two functions of carrier generation and carrier movement are expected to be separated spatially in a lattice. Based on the concept of spatial separation, Kawazoe and co-workers studied the transparency and conductivity of

some complex oxides, including  $\text{MgIn}_2\text{O}_4$ ,<sup>6</sup>  $\text{ZnGa}_2\text{O}_4$ ,<sup>7</sup> and  $\text{Y}_2\text{Sb}_2\text{O}_7$ .<sup>8</sup> They found that these oxides are transparent conductors, and suggested that the chain structure of the edge sharing  $\text{MO}_6$  octahedra, where  $M$  is a  $p$ -block metal ion surrounded by six oxygen ions, might serve as a path for electrons, thereby facilitating electrical conductivity. They have suggested that the other sites containing metal ions or vacant spaces outside the chains in the complex oxides could serve as sites for dopant ions due to the fact that they are separated from the space in which the conductive electrons move. However, no study has been reported so far on effective dopant ions or changes in carrier density and mobility due to concentrations of the dopant ions.

$\text{InGaZnO}_4$  is one of the complex oxides that has the structure of the edge-sharing  $\text{MO}_6$  octahedra. It is an  $\text{YbFe}_2\text{O}_4$ -type layered structure with alternating laminated layers of  $\text{YbO}_2$  and  $\text{Fe}_2\text{O}_2$ .<sup>9</sup> In the case of  $\text{InGaZnO}_4$ ,  $\text{InO}_2$  substitutes for the  $\text{YbO}_2$  layers, and  $\text{GaZnO}_2$  layers replace the  $\text{Fe}_2\text{O}_2$  layers (Fig. 1).<sup>10</sup> These layers accumulate in the following order:  $\text{InO}_2$ ,  $\text{GaZnO}_2$ ,  $\text{GaZnO}_2$ ,  $\text{InO}_2$ ,  $\text{GaZnO}_2$ ,  $\text{GaZnO}_2$ ,  $\text{InO}_2$ ,  $\text{GaZnO}_2$ , and  $\text{GaZnO}_2$ . That is, three  $\text{InO}_2$  layers and three pairs of  $\text{GaZnO}_2$  layers accumulate alternatively to form one unit cell. Since the  $\text{InO}_2$  layer is composed of edge-sharing oxygen octahedra centered by In ions, it could serve as a path for carrier electrons. It is also possible that the  $\text{GaZnO}_2$  layer could serve as a carrier path, due to the fact that the local structure around the Zn ions is similar to that of  $\text{ZnO}$ , which is well known to be a transparent conductor. The conductivity and transparency of  $\text{InGaZnO}_4$  have been confirmed using sintered bodies<sup>11</sup> and thin-film specimens on quartz glass substrates deposited by a conventional rf magnetron sputtering method.<sup>12</sup> Thin-film speci-

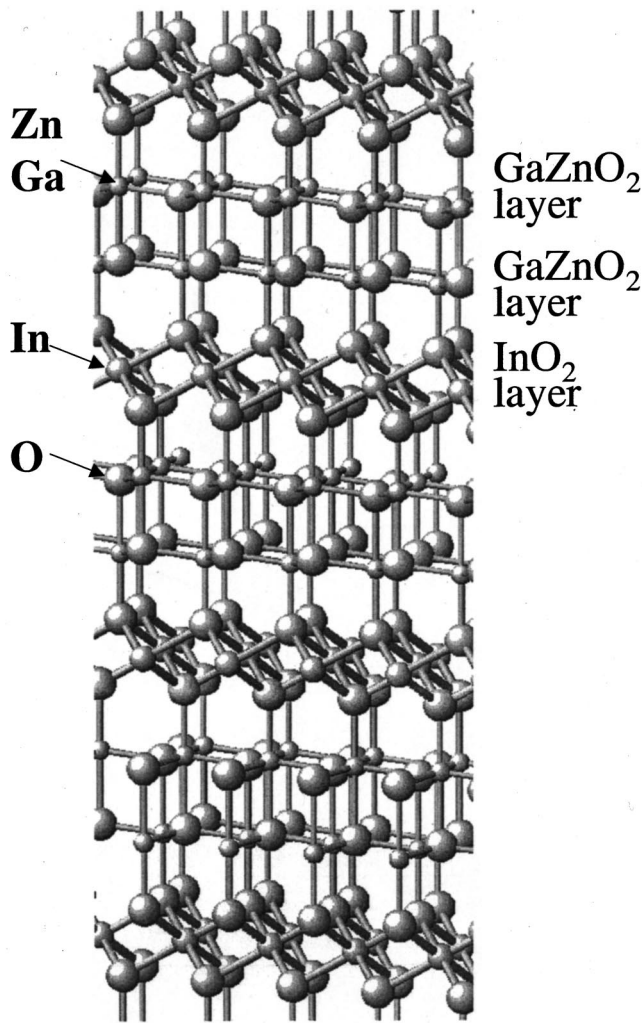


FIG. 1. Crystal structure of  $\text{InGaZnO}_4$ .

mens had a carrier density of  $1.2 \times 10^{20}/\text{cm}^3$ , a mobility of  $24 \text{ cm}^2/\text{V s}$ , and a conductivity of  $500 \text{ S/cm}^2$  (Table I). The carrier density is comparable to that of an  $\text{In}_2\text{O}_3$  film deposited by an electron beam evaporation method.<sup>3</sup> The donor states in the  $\text{InGaZnO}_4$  films are considered to be due to oxygen defects, and are expected to be increased by the introduction of an appropriate dopant, as in the case of  $\text{In}_2\text{O}_3$ , which uses Sn as a dopant. The table shows that the carrier density of a commercial ITO film was measured to be  $1.4 \times 10^{21}/\text{cm}^3$ . Such heavy doping in the  $\text{InGaZnO}_4$  lattice may result in a conductivity greater than that of ITO, since elimination of the oxygen defect, which should disturb the conduction, and

TABLE I. Electrical and optical properties of an  $\text{InGaZnO}_4$  sputtered film with those of an  $\text{In}_2\text{O}_3$  film deposited by an electron beam evaporation method (Ref. 3) and an ITO film commercially produced.

	$\text{InGaZnO}_4$	$\text{In}_2\text{O}_3$	ITO
Band gap (eV)	3.5	3.2	3.2
Conductivity S/cm	$5.0 \times 10^2$	$1.7 \times 10^3$	$7.0 \times 10^3$
Mobility ( $\text{cm}^2/\text{V s}$ )	24	130	30
Carrier density ( $\text{S/cm}^3$ )	$1.2 \times 10^{20}$	$0.8 \times 10^{20}$	$1.4 \times 10^{21}$

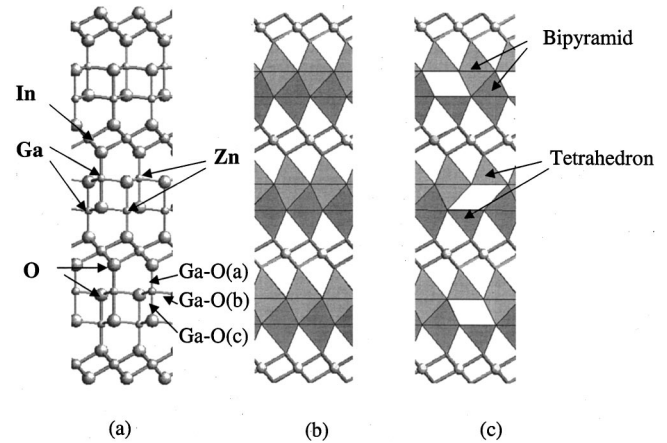


FIG. 2. Simplified crystal structure with polyhedral models. (a) Balls and sticks model, (b) polyhedrons in nonrelaxed structure, (c) polyhedrons in relaxed structure.

doping with the ion substitution at appropriate sites may result in an enhancement not only in carrier density but also in mobility.

In order to realize such a high conductivity in an  $\text{InGaZnO}_4$  system based on the concept of spatial separation, it is important to specify the paths of conductive electrons in the lattice. If the  $\text{InO}_2$  layers work as the conduction paths, dopant ions should be introduced at the sites of Ga or Zn ions. On the other hand, if the  $\text{ZnGaO}_2$  layers serve as the conduction paths, In ions should be substituted with some dopant ions. In this paper, in order to specify the conduction paths of electrons in the  $\text{InGaZnO}_4$  lattice, the electronic structure of the crystal was calculated based on discrete-variational (DV)  $X\alpha$  theory using cluster models.

## II. MODELS AND CALCULATIONS

Because the precise crystal structure of  $\text{InGaZnO}_4$  has not yet been clarified, the positions of atoms were derived from the lattice parameters of  $\text{InGaZnO}_4$  (Ref. 10) and the fractionally coordinated atomic positions in  $\text{YbFe}_2\text{O}_4$ , as shown in Fig. 1.<sup>9</sup> As the crystal structure is complicated, a simplified view is shown in Fig. 2(a). Five oxygen ions surround a Ga or Zn ion to form a trigonal bipyramidal  $\text{MO}_5$ . A polygon model is used to show the bipyramids in the  $\text{GaZnO}_2$  layers in Fig. 2(b). The bipyramidal polygons connect with each other at the corners to form a  $\text{GaZnO}_2$  layer (shaded darker), on which there is another  $\text{GaZnO}_2$  layer (shaded brighter). Ga and Zn are located at an identical site at the center of the bipyramids.

Regarding the chemical bond, however, the bond lengths of Ga-O and Zn-O should be different, and this could result in some differences in electronic structure. In order to obtain a reasonable crystal structure, relaxation calculations using classical two-center potentials were performed using the General Utility Lattice Program (GULP).<sup>13</sup> Forces are assumed to be of the two-body type, and a function only of the distance between atoms. The interatomic interactions are divided into long-range Coulombic and short-range forces, with the short-range term described using the following analytical function:

TABLE II. Parameters used for optimization of atom positions in the InGaZnO<sub>4</sub> lattice using the two-center potential of scheme 1 in the text.

Interaction type	A (eV)	$\rho$ (Å)	C (eV Å <sup>-6</sup> )
In <sup>3+</sup> —O <sup>2-</sup>	1293.600	0.331	4.325
Zn <sup>2+</sup> —O <sup>2-</sup>	600.300	0.337	0.000
Ga <sup>2+</sup> —O <sup>2-</sup>	2339.766	0.274	0.000
O <sup>2-</sup> —O <sup>2-</sup>	25.410	0.694	32.320

$$\phi_{ij}(r) = A_{ij} \exp\left(\frac{-r}{\rho_{ij}}\right) - \frac{C_{ij}}{r^6}, \quad (1)$$

where  $A_{ij}$ ,  $\rho_{ij}$ , and  $C_{ij}$  are parameters particular to each ion-ion interaction. Parameters determined by Bush *et al.*<sup>14</sup> and Fisher *et al.*,<sup>15</sup> as listed in Table II, were used.

For the nonrelaxed and relaxed crystal structure, nonrelativistic first-principles molecular orbital (MO) calculations were made by the DV- $X\alpha$  method<sup>16,17</sup> using the SCAT program.<sup>17</sup> MO were constructed by linear combination of atomic orbitals (AO) as

$$\phi_l(r_k) = \sum_i C_{il} \chi_i(r_k), \quad (2)$$

where  $\chi_i(r)$  is the AO and  $r_k$  is one of the sampling points in the DV calculation. The number of sampling points was set at 1400 per atom. The numerical basis functions were obtained by solving the radial part of the Schrödinger equations. Minimal basis sets of  $1s-2p$  for O;  $1s-3d, 4s$ , and  $4p$  for Zn and Ga; and  $1s-4d, 5s$ , and  $5p$  for In were used.

Overlap population is a useful characteristic to examine when studying the interactions between orbitals, though it is inherently arbitrary. The overlap population between the  $i$ th AO and the  $j$ th AO at the  $l$ th MO is given by

$$Q_{ij}^l = C_{il} C_{jl} \sum_k \omega(r_k) \chi_i(r_k) \chi_j(r_k), \quad (3)$$

where  $\omega(r)$  is the integration weight or reciprocal of the sample point density at  $r_k$ . The sum of  $Q_{ij}^l$  with respect to  $l$  for occupied orbitals provides the net overlap population between the  $i$ th AO and  $j$ th AO; in other words,

$$Q_{ij} = \sum_{l}^{\text{occupied}} Q_{ij}^l. \quad (4)$$

TABLE III. Bond lengths between metals and oxygens in the InGaZnO<sub>4</sub> lattice.

Metal	Bond type	Bond length	
		nonrelaxed	relaxed
In		2.180	2.136, 2.243
Ga	<i>a</i>	2.020	1.904
	<i>b</i>	1.923	1.908, 1.949
	<i>c</i>	2.237	2.080
Zn	<i>a</i>	2.020	2.063
	<i>b</i>	1.923	1.913, 1.963
	<i>c</i>	2.237	2.425

TABLE IV. Orbital energies of ions isolated, in Madelung fields of the nonrelaxed and relaxed crystal structure.

Orbital	Energy		
	isolated	nonrelaxed	relaxed
O $2p$	19.4	-5.3~3.3	-4.8~4.0
Zn $4s$	-21.0	5.8	4.2
In $5s$	-30.8	0.5, 0.9	0.5, 1.5
Ga $4s$	-34.8	-1.4	0.2

The overlap population between atoms  $A$  and  $B$  is given by

$$Q_{AB}^l = \sum_{i \in A} \sum_{j \in B} Q_{ij}^l. \quad (5)$$

Diagrams of overlap population are made by broadening  $Q_{AB}^l$  at individual MO's using Gaussian functions of 1.0-eV full width at half maximum.

### III. RESULTS AND DISCUSSION

Bond lengths between metal and oxygen ions in the lattice, which were derived from the lattice constants of InGaZnO<sub>4</sub> crystal and the fractional atomic positions in YbFe<sub>2</sub>O<sub>4</sub> crystal, are listed in Table III. There are three Ga (Zn)-O bonds between the central Ga (Zn) ion and the three oxygen ions at the corners of the basal triangle of the bipyramid [Ga (Zn)-O (*b*)], and two bonds between the Zn (Ga) and O ion at the top of the pyramid of the InO<sub>2</sub> layer side [Ga (Zn)-O (*a*)] and that of the GaZnO<sub>2</sub> layer side [Ga (Zn)-O (*c*)] [Fig. 2(a)]. The reported bond lengths between O ions and Ga ions with hexagonal coordination in various oxides vary from 1.940 to 2.077 Å,<sup>18</sup> and that of Zn-O with tetrahedral coordination have values between 1.973 and 1.992 Å.<sup>18</sup> The bond lengths derived for the nonrelaxed structure have abnormal values for Ga-O (*c*) and Zn-O (*c*).

The relaxed structure of the crystal was calculated under

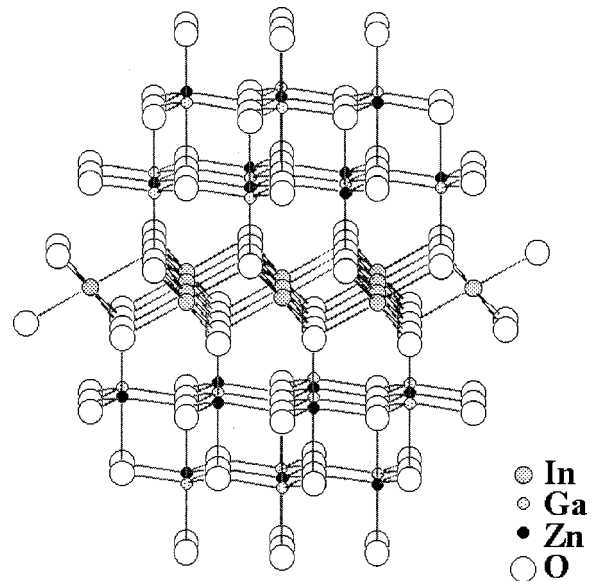


FIG. 3. In<sub>3</sub>Ga<sub>20</sub>Zn<sub>18</sub>O<sub>118</sub> cluster model used for electronic calculations.

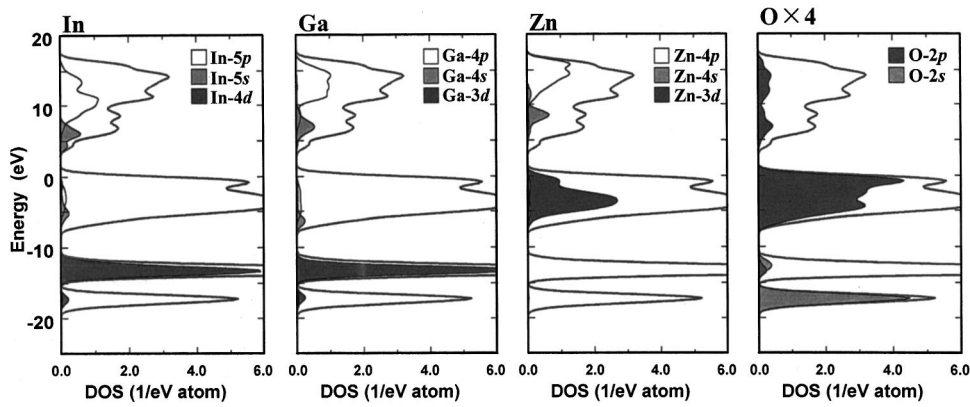


FIG. 4. Partial DOS curves for relaxed crystal structure.

certain restrictions using GULP. The lattice constants were fixed at the values from experimental data reported for a  $\text{InGaZnO}_4$  crystal. The  $X$  and  $Y$  values used as Cartesian coordinates for all the atoms and lattice constants were fixed, while the  $Z$  values were optimized due to the fact that the bonds  $\text{Zn-O}$  ( $c$ ) and  $\text{Ga-O}$  ( $c$ ) are parallel to the  $Z$  axis. Restriction by inversion symmetry was also applied. The arrangement of Ga and Zn ions on the  $\text{GaZnO}_2$  layer has been considered to be random by Li *et al.*,<sup>19</sup> since no extra diffraction spots were formed in x-ray diffraction patterns. Calculations with some arrangement of Ga and Zn ions were performed, and no significant difference was seen in the results of the structural relaxation and electronic state. The bond lengths following the optimization are also listed in Table III. In-O bond lengths resulted in two different values, reflecting the existence of two types of oxygen ions in the  $\text{InO}_2$  layer. The bond lengths of Ga-O ( $b$ ) and Zn-O ( $b$ ) changed into two values as well, due to the fact that there are two types of oxygen ions based on the number of Ga and Zn neighbors in the  $\text{GaZnO}_2$  layer. The length of Ga-O ( $c$ ) reduced to a reasonable value of 2.080 Å. The length of Zn-O ( $c$ ) changed to 2.425 Å, which suggests that the Zn ions lost the vertical bonds of Zn-O ( $c$ ), and have tetrahedral coordination as shown in Fig. 2(c). It was recently reported that Zn has tetrahedral coordination in  $\text{In}_2\text{O}_3$  ( $\text{ZnO}$ ) <sub>$m$</sub>  layered materials, which has a homologous structure of  $\text{InGaZnO}_4$ .<sup>19</sup>

The change in the atomic position had some effect on the electronic structure mainly through changes in the Madelung potential. The orbital energies of isolated ions of  $\text{In}^{3+}$ ,  $\text{Ga}^{3+}$ ,  $\text{Zn}^{2+}$ , and  $\text{O}^{2-}$ , as calculated using the SCAT program, are listed in Table IV. The orbital with the highest energy is O  $2p$ , that of metal ions is Zn  $4s$ , and the lowest level is Ga  $4s$ . When the ions are positioned at the sites of each ion in a  $\text{InGaZnO}_4$  crystal with a nonrelaxed structure, the energies of orbitals are greatly affected by the Madelung poten-

tial. O  $2p$  came to have the lowest energy of all the levels, and Zn  $4s$  moved to the highest position. The energy of In  $5s$  also changed, becoming slightly higher than that of Ga  $4s$ . This simple ionic model indicates that the conduction-band edge of the nonrelaxed structure is formed by the Ga  $4s$  level. In the case of the relaxed structure, the energies of In  $5s$  and Ga  $4s$  are close because the energy of In  $5s$  was not altered while that of Ga  $4s$  was increased by 1.6 eV. The main reason for the shift in Ga  $4s$  is undoubtedly related to the change in the bond length between Ga and O. Relaxation reduced the distances [7% in the case of Ga-O ( $c$ )], which in turn increased the static potential at the Ga site. On the other hand, the bond lengths between In and O did not change significantly (less than 2%).

Electronic state calculations were performed using a cluster of  $\text{In}_{13}\text{Ga}_{20}\text{Zn}_{18}\text{O}_{118}$  as a model for the crystal (Fig. 3). An  $\text{InO}_2$  layer is laminated with two  $\text{GaZnO}_2$  layers on both sides. The cluster was embedded in the Madelung potential generated by point charges. In order to analyze the origins of the conduction band and valence band, a series of eigenvalues for molecular orbitals were obtained using DV- $X\alpha$  calculations, and the eigenvalues were broadened by Gaussian functions for 0.5-eV full width at half maximum (FWHM) to obtain the total and partial density of states (DOS) state curves. Since a set of molecular orbitals is often referred to as a band, in the descriptions below the set of molecular orbitals corresponding to a certain partial DOS curve is noted as a partial band. Differences in the DOS curves for the nonrelaxed and relaxed structure were little and not important, and that for the relaxed structure are plotted in Fig. 4. The zero point on the vertical energy axis was adjusted to the highest occupied molecular orbital (HOMO) of the cluster. The top of the valence band is located at zero energy because the valence band is fully occupied by electrons while the conduction band is empty. The valence band is formed pri-

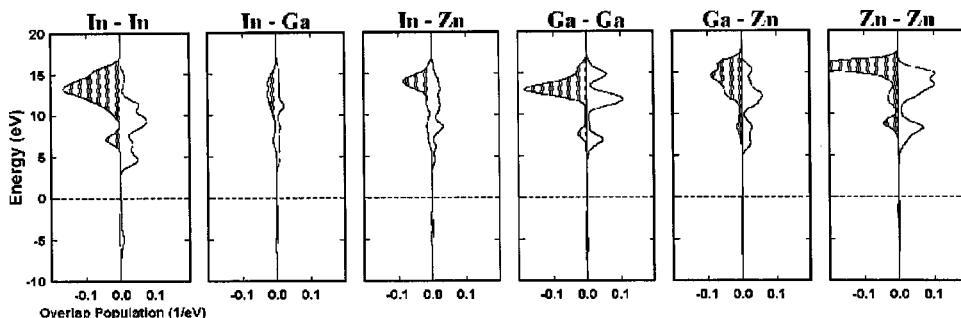


FIG. 5. Overlap population curves for relaxed crystal structure.

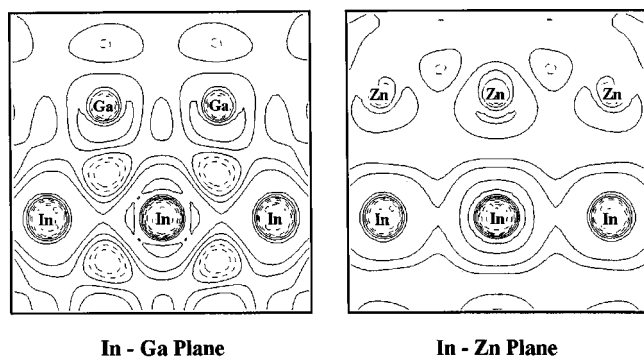


FIG. 6. Contour maps of the level at the edge of the conduction band.

marily by O  $2p$  and Zn  $3d$  partial bands. The gap between the HOMO and lowest unoccupied molecular orbitals (LUMO), which corresponds to the band gap, is 4.4 eV, which was appreciably greater than the experimental value of 3.5 eV (see Table I). The primary reason for the wider band gap may be the limited size of the cluster, as reported in the case of DV- $X\alpha$  calculations for  $\text{In}_2\text{O}_3$  systems.<sup>20</sup> The conduction band is formed by the curves of the  $s$  and  $p$  orbitals of the three metals, with some influence by the O  $2p$  curve. The In  $5s$  partial DOS has a shoulder peak on the lower-energy side. Ga  $4s$  has a single peak whose energy is more than 2 eV higher from the edge of the conduction band. The base of the Zn  $4s$  main peak is 3.4 eV higher than the band edge. The bottom of the conduction band is then formed by the In  $5s$  band only. The order of In  $5s$  and Ga  $4s$  differs from that of the simple ion model in Table IV. In the ionic model, the lowest unoccupied orbital was Ga  $4s$ , and In  $5s$  was slightly above that. The DOS curves indicate that electronic interaction reduces the energy of In  $5s$  to less than that of Ga  $4s$ .

The characteristics of the electronic interaction can be studied by overlap population analysis. The distribution of overlap populations between two metal ions is plotted in Fig. 5. The positive and negative values of the population indicate bonding and antibonding characteristics of the interactions between two atomic orbitals. At the bottom of the conduction band, the In-In bonding population is dominant, indicating that the electronic interaction that stabilizes the energy of the In  $5s$  partial band is due to In-In bonding. The peak of the Ga-Ga bonding population is slightly higher than the In-In bonding peak. A peak for Ga-Zn is also seen at the same energy region. The Ga-Zn population has another peak 3.4-eV higher than the band edge, where a Zn-Zn peak is also seen. These characteristics indicate significant interactions between metals in the  $\text{InO}_2$  layer and those in the  $\text{GaZnO}_2$  layer. On the other hand, the populations of In-Ga and In-Zn, which correspond to interactions across the layers, are very small along the entire energy axis. The electronic structure of  $\text{InGaZnO}_4$  has strong two-dimensional characteristics, reflecting its crystal structure, and this implies that In  $5s$ , Ga  $4s$ , or Zn  $4s$  bands localize in the  $\text{InO}_2$  layer or  $\text{GaZnO}_2$  layer.

The electrons in the donor levels just below the conduction-band edge can be excited up to conduction band at room temperature and made to display electrical conductivity. Since the edge of the conduction band is formed by the In  $5s$  band, it is thought that the In  $5s$  band provides a

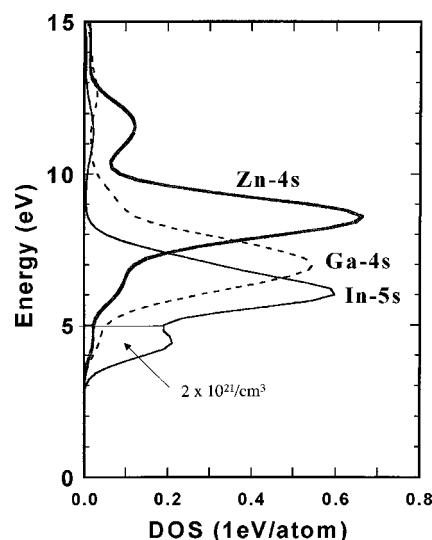


FIG. 7. Partial DOS curves in the conduction band of the relaxed structure, magnified from Fig. 4.

path for electrical conductivity in the crystal, that is, the  $\text{InO}_2$  layers should serve as conduction paths. The spatial distribution of the In  $5s$  band can be seen in contour maps of the wave functions of the original molecular orbitals. Figure 6 shows the wave function for the LUMO, which corresponds to the edge of the conduction band. The wave function was displayed along two planes on which a chain of In ions is located. A chain of Ga ions or Zn ions is also seen on the In-Ga and In-Zn planes, respectively. It can be seen that the wave functions of In  $5s$  orbitals overlap each other with the same phase, localizing along the In chain.

In the case of a heavily doped system, the possibility that the Ga  $4s$  band also works as a carrier path should be discussed. For film specimens with a carrier density of  $1 \times 10^{21}/\text{cm}^3$ , the Fermi level of the  $\text{InGaZnO}_4$  film specimens would be located 1-eV higher than the edge of the conduction band (this value being estimated based on data on the Burstein-Moss shift of the absorption edge as a function of carrier density).<sup>12</sup> Since the base of the Ga  $4s$  partial band is located 2-eV higher than the band edge, as shown in Fig. 7 of a magnified version of the DOS curves for the conduction band given in Fig. 4, which in turn has twice as much energy as the shift, and because the number of states of the In  $5s$  band under the edge of the Ga  $4s$  band is estimated to be  $2 \times 10^{21}/\text{cm}^3$  (electron density:  $4 \times 10^{21}/\text{cm}^3$ ) based on the area of the curve and the density of In atoms, the Ga  $4s$  band may not play an important role even in such a heavily doped system. Furthermore, the Zn  $4s$  band is not likely to serve as a conduction path, as its energy is far higher. Surprisingly, although ZnO has great conductivity comparable to  $\text{In}_2\text{O}_3$ , the Zn  $4s$  orbitals in  $\text{InGaZnO}_4$  do not play an important role in the electrical conductivity. The  $\text{ZnGaO}_2$  layers thus do not serve as conduction paths.

Since the In  $5s$  band is the only band to serve as a conduction path, dopant ions in the  $\text{GaZnO}_2$  layers may play little or no part in scattering electrons that move within the  $\text{InO}_2$  layer. In other words, in a system heavily doped by substituted ions, the reduction in mobility is restrained. Experimental research is underway on the relationship between

the electrical properties of polycrystalline specimens and the concentration of dopant ions.

#### IV. CONCLUSION

The electronic structure of  $\text{InGaZnO}_4$  with a  $\text{YbFe}_2\text{O}_4$ -type crystal structure was calculated by the DV- $X\alpha$  method in order to study the mechanism of electrical conductivity. A reasonable crystal structure was obtained using the GULP program to perform relaxation calculations with classical two-center potentials. While Ga retained pentagonal coordination bonding to three oxygen ions at the corners of a basal triangle and two oxygen ions at the tops of the two pyramids, Zn had tetragonal coordination, with a missing bond between Zn and oxygen at the top of one of the pyramids.

The electronic structure of the relaxed  $\text{InGaZnO}_4$  crystal was two dimensional. The electronic state at the edge of the

conduction band was formed by overlapping between In  $5s$  orbitals, which delocalize in the  $\text{InO}_2$  layer. The energies of the Ga  $4s$  and Zn  $4s$  bands were too high for those bands to be doped with electrons. The In  $5s$  band may be mainly occupied by the electrons and work as conduction paths even in a heavily doped system. The spatial separation effect, that is, the restraining of a reduction in mobility under a high concentration of dopant ions, can be expected, since the dopant ions introduced in the  $\text{GaZnO}_2$  layers may have little effect in scattering carriers in the  $\text{InO}_2$  layers.

#### ACKNOWLEDGMENTS

The authors would like to thank Dr. J. D. Gale for allowing us to use the GULP program, Professor N. Kimizuka at Sonora University for useful comments and suggestions, and F. Ohba at Kyoto University and H. Ohta of HOYA Corporation for their help in this study.

- 
- <sup>1</sup>J. C. C. Fan and J. B. Goodenough, *J. Appl. Phys.* **48**, 3524 (1977).
- <sup>2</sup>R. L. Weiher, *J. Appl. Phys.* **33**, 2834 (1962).
- <sup>3</sup>Y. Shigesato and D. C. Paine, *Appl. Phys. Lett.* **62**, 1268 (1993).
- <sup>4</sup>S. Ishibashi, Y. Higuchi, Y. Ota, and K. Nakamura, *J. Vac. Sci. Technol. A* **8**, 1403 (1990).
- <sup>5</sup>H. Kawazoe, N. Ueda, H. Un'no, T. Omata, H. Hosono, and H. Tanoue, *J. Appl. Phys.* **76**, 7935 (1994).
- <sup>6</sup>H. Un'no, N. Hikuma, T. Omata, N. Ueda, T. Hashimoto, and H. Kawazoe, *Jpn. J. Appl. Phys., Part 2* **32**, L1260 (1993).
- <sup>7</sup>T. Omata, N. Ueda, K. Ueda, and H. Kawazoe, *Appl. Phys. Lett.* **64**, 1077 (1994).
- <sup>8</sup>K. Yanagawa, Y. Ohki, T. Omata, H. Hosono, N. Ueda, and H. Kawazoe, *Appl. Phys. Lett.* **64**, 2071 (1994).
- <sup>9</sup>K. Kato, I. Kawada, N. Kimizuka, and T. Katsura, *Z. Kristallogr.* **141**, 314 (1975).
- <sup>10</sup>N. Kimizuka and T. Mohri, *J. Solid State Chem.* **60**, 382 (1985).
- <sup>11</sup>M. Orita, M. Takeuchi, H. Sakai, and H. Tanji, *Jpn. J. Appl. Phys., Part 2* **34**, L1550 (1995).
- <sup>12</sup>M. Orita, H. Sakai, M. Takeuchi, and Y. Yamaguchi, *Trans. Mater. Res. Soc. Jpn.* **20**, 573 (1996).
- <sup>13</sup>J. D. Gale, *J. Chem. Soc., Faraday Trans.* **93**, 629 (1997).
- <sup>14</sup>T. S. Bush, J. D. Gale, C. R. A. Catlow, and P. D. Battle, *J. Mater. Chem.* **4**, 831 (1994).
- <sup>15</sup>C. A. J. Fisher, M. S. Islam, and R. J. Brook, *J. Solid State Chem.* **128**, 137 (1997).
- <sup>16</sup>H. Adachi, M. Tsukada, and C. Satoko, *J. Phys. Soc. Jpn.* **45**, 875 (1978).
- <sup>17</sup>D. E. Ellis, H. Adachi, and F. W. Averill, *Surf. Sci.* **58**, 497 (1976).
- <sup>18</sup>A. F. Wells, *Structural Inorganic Chemistry*, 5th ed. (Oxford, New York, 1984), Chap. 12, p. 531.
- <sup>19</sup>C. Li, Y. Bando, M. Nakamura, and N. Kimizuka, *J. Electron Microsc.* **46**, 119 (1997).
- <sup>20</sup>I. Tanaka, M. Mizuno, and H. Adachi, *Phys. Rev. B* **56**, 3536 (1997).